

# Development of a Precise Docking System for Large City Buses

K. OKADA M. NAKA S. KAWAHARA

*We developed a precise docking control technology for large city buses as projects promoted by Japan's Cabinet Office. Precise docking technology is a technology to minimize the gap between the step of the bus and the platform at a bus stop, and is necessary for smooth boarding/alighting and on-time performance. We installed steering and braking control systems, and developed control strategy. First, we constructed a steering and braking algorithm. This report introduces precise docking technology and evaluation in traffic environment.*

**Key Words:** steering control, autonomous driving, precise docking, path following control, large vehicle

## 1. Introduction

In recent years, technology development related to autonomous driving has been actively promoted. In Japan, the Cabinet Office works with relevant ministries and agencies to promote the Cross-ministerial Strategic Innovation Promotion Program - Automated Driving for Universal Services (SIP-adus), and various projects are being carried out for the practical application of autonomous driving systems<sup>1)</sup>.

One of the benefits expected of autonomous driving is its use in public transportation. While it is estimated that the demand for public transportation will increase as a means of transportation for the elderly as declining birthrate and aging, the shortage of bus drivers due to aging has become a major problem. In order to improve this situation, development aimed at utilizing autonomous driving in buses is being promoted by various organizations. JTEKT has been consigned with projects of the SIP-adus relating to bus autonomous driving for solving the abovementioned issues, namely; "Investigation about actuators and control for advanced rapid transit system in investigation and consideration about issues towards autonomous driving system"<sup>2)</sup>, "Next generation transport Development of sensing and control technology for Docking of Advanced Rapid Transit system,"<sup>3), 4)</sup> and "Investigation concerning automated driving bus in Okinawa"<sup>5)</sup>, and has been engaging in R&D activities accordingly.

This paper will report the autonomous driving technology for large buses developed in these consigned projects. The following content was based on reports of these projects.

## 2. About the Consignment Projects

In relation to the autonomous driving of large buses, JTEKT was consigned with "Strategic Innovation Promotion Program (SIP) Automated driving systems/Field operational test/Next generation transport Development of sensing and control technology for Docking of Advanced Rapid Transit system" and "Investigation concerning automated driving bus in Okinawa," and has been carrying out R&D accordingly.

In this program, we have been developing the next generation transport system "Advanced Rapid Transit (ART)," which is easy for a wide range of people to use, including the elderly and others with mobility limitations by leveraging autonomous driving technology. In ART, we aim for the smooth boarding and alighting of buses without assistance, even for users in wheelchairs, for example. As a result, we aim to realize the timely operation of buses. The technology required to achieve these goals is precise docking technology which ensures that the bus stops accurately at a bus stop with minimal gap. In the "Development of sensing and control technology for Docking of Advanced Rapid Transit system," JTEKT developed a technology for precise docking in large buses. In this project, we conducted a large-scale field operational test in the Tokyo Bay Area to verify the precise docking technology. **Figure 1** shows the experiment course. Precise docking was performed in four places indicated by the circles in the figure.

In addition, for the implementation of elemental technologies developed in ART, it is important to verify technical issues through experiments under various environments and conditions as well as widely promote its convenience. As part of this effort, the Cabinet Office has conducted an experiment of buses utilizing autonomous driving technology in Okinawa Prefecture, which has

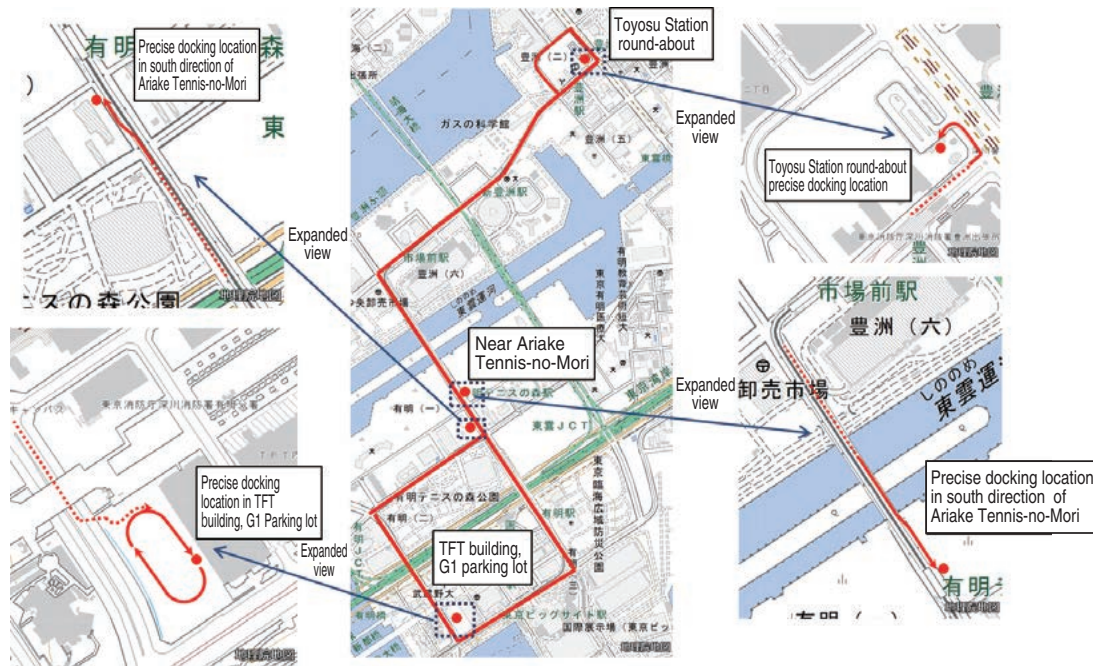


Fig. 1 Experiment course (Tokyo Bay area)

\* This map is created by JTEKT Corporation based on “GSI maps” published by the Geospatial Information Authority of Japan.

various traffic problems such as traffic congestion due to traffic concentration and the weakness of transportation in depopulated areas. Regarding the “Investigation concerning automated driving bus in Okinawa”, in order to verify the possibility of utilizing autonomous driving technology in the local traffic environment, we developed a driving technology on a large bus, and verified the social acceptability of bus operators and general users. **Figure 2** shows the route used for the Okinawa experiment. It was carried out along a route including main roads with a large volume of traffic connecting Naha Airport, the outlet mall in Tomigusuku City, and the roadside station, Toyosaki. In addition, automatic control of steering and braking was performed at the place where precise docking and deceleration control are displayed in the figure, and automatic control of steering was performed on the other routes except for a part. In the test ride by general users, approximately 1 200 people rode the bus as passengers through a duration of 14 days.



Fig. 2 Experiment route (Okinawa)

In this paper, we report the control technology (precise docking technology) of autonomous driving developed in these consigned projects. In the projects, in addition to autonomous driving technology, we conducted peripheral recognition technology using cameras, LiDAR (Light Detection And Ranging), cooperation technology with drivers, and evaluation of quasi-zenith satellite positioning accuracy, however reports on the performance of these are omitted here. Details of the information can be found on the Cabinet Office website<sup>4), 5)</sup>.

### 3. System Configuration

#### 3.1 Experimental Vehicle System Configuration

Figure 3 shows the appearance of the experimental vehicle used in this development, while Table 1 shows vehicle specifications. The weight is the value measured when one driver is riding in the vehicle. This vehicle is equipped with sensing systems for recognizing the vehicle position and surrounding environment, and control systems that can control steering and braking. Figure 4 shows the overall configuration of the control system. Control operations are performed by the integrated control system. The GNSS (Global Navigation Satellite System) receiver is used to detect vehicle position. Control using distance information to the white line obtained by the camera is also possible. The vehicle angle and angular velocity obtained from the gyro sensor built into the GNSS receiver are also used for control. Target steering angle and target deceleration calculated by the integrated control system are instructed to the steering control ECU and the braking control ECU, respectively.

**Table 1** Major specifications of experimental vehicle

Item	Unit	Value
Length/ Width/ Height	mm	10 555 / 2 485 / 3 105
Wheel base	mm	5 300
Tread	mm	Front: 2 065, Back: 1 820
Weight (axle load)	kg	Front: 3 163, Back: 6 607

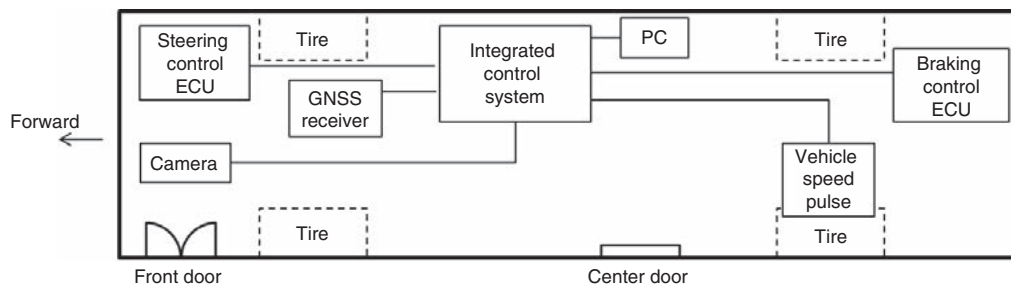
#### 3.2 Steering and Braking Control System

Figure 5 shows the conceptual diagram of the steering control system. The steering mechanism is ball-screw hydraulic power steering, and its function is maintained, while a steering actuator is mounted on the steering column. In this development, automatic steering was realized by giving the steering actuator the target steering angle.

Figure 6 shows the conceptual diagram of the braking control system. An electronically controlled brake system was installed to enable external control. The braking control ECU receives the target deceleration from the integrated control system, calculates the air pressure for the front axle and the rear axle, and instructs the braking control actuator to achieve the required deceleration.



**Fig. 3** Appearance of experimental vehicle



**Fig. 4** Control system configuration

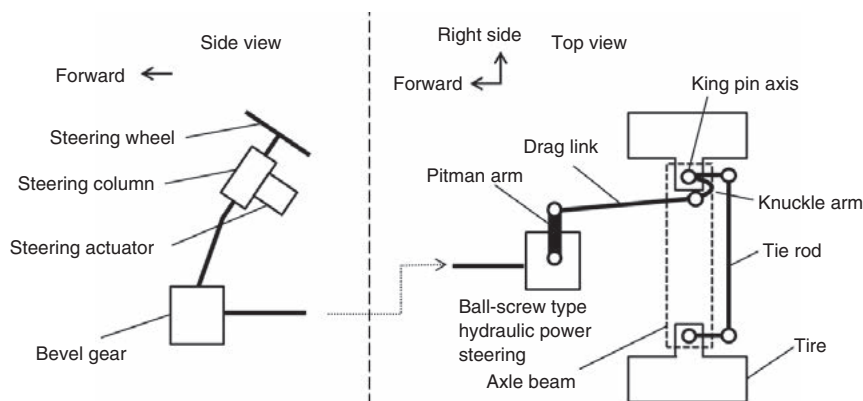


**Fig. 5** Concept of steering system configuration

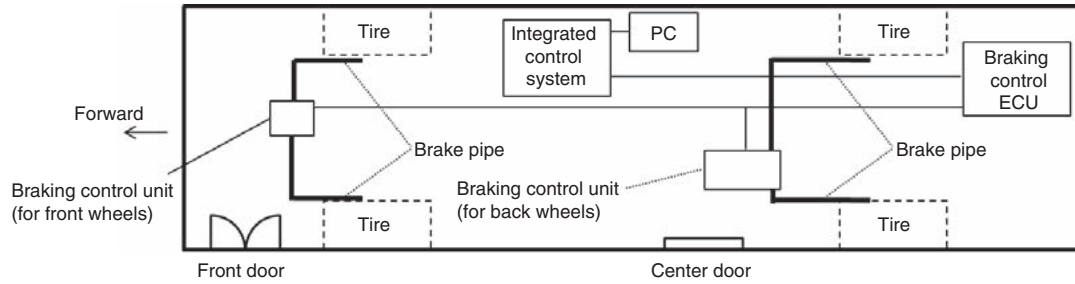


Fig. 6 Concept of braking system configuration

### 4. Precise Docking Technology

The “precise docking” which ensures a bus stops accurately with minimal gap between the bus entrance and bus stop requires technology to stop the vehicle accurately both in the longitudinal direction and the lateral direction with respect to the target stop position. This Section describes the calculation of the target steering angle in the steering control for lateral direction and the calculation of the target deceleration in the braking control for longitudinal direction.

#### 4.1 Steering Control

A single track model (Fig. 7) was selected as the vehicle motion model used for steering control system design. Vehicle dynamics are expressed in (1), (2).

$$\frac{d}{dt} \begin{bmatrix} \gamma \\ \beta \end{bmatrix} = A \begin{bmatrix} \gamma \\ \beta \end{bmatrix} + B\delta \tag{1}$$

$$A = \begin{bmatrix} a_{11} & a_{12} \\ a_{21} & a_{22} \end{bmatrix} = \begin{bmatrix} -\frac{2}{JV} (K_f l_f^2 + K_r l_r^2) & -\frac{2}{J} (K_f l_f - K_r l_r) \\ -\frac{2}{MV^2} (K_f l_f - K_r l_r) - 1 & -\frac{2}{MV} (K_f + K_r) \end{bmatrix},$$

$$B = \begin{bmatrix} b_{11} \\ b_{21} \end{bmatrix} = \begin{bmatrix} \frac{2}{J} K_f l_f \\ \frac{2K_f}{MV} \end{bmatrix} \tag{2}$$

Whereby  $V$ : vehicle velocity,  $M$ : vehicle mass,  $\beta$ : slip angle,  $\gamma$ : yaw rate around the center of gravity,  $F_f, F_r$ : lateral force of the tire on the front and rear wheels,  $l_f, l_r$ : Distance from center of gravity to front and rear tire axles,  $J$ : moment of inertia around the center of gravity,  $K_f, K_r$ : cornering stiffness of the front and rear tires.

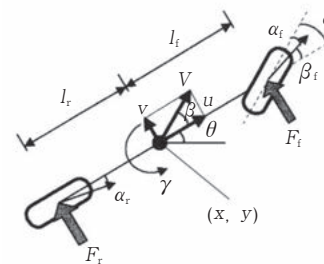


Fig. 7 Single track model

To calculate the target steering angle in steering control, Path Following control to follow the trajectory of the reference vehicle traveling on a virtual reference track, i.e. target trajectory, was used, as shown in Fig. 8<sup>2),6)</sup>.

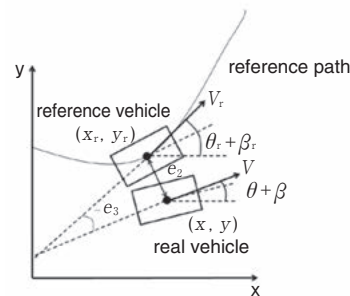


Fig. 8 Path Following control

When the coordinates and the yaw angle deviation of the real vehicle with respect to the reference vehicle are defined as  $e_1, e_2,$  and  $e_3$ , the following equation is established. In this equation, the subscript  $r$  represents variables of the reference vehicle.

$$\begin{bmatrix} e_1 \\ e_2 \\ e_3 \end{bmatrix} = \begin{bmatrix} \cos(\theta_r + \beta_r) & \sin(\theta_r + \beta_r) & 0 \\ -\sin(\theta_r + \beta_r) & \cos(\theta_r + \beta_r) & 0 \\ 0 & 0 & 1 \end{bmatrix} \begin{bmatrix} x - x_r \\ y - y_r \\ (\theta + \beta) - (\theta_r + \beta_r) \end{bmatrix} \tag{3}$$

Assuming the reference vehicle velocity aligns with that of the real vehicle and the two vehicles are constantly travelling parallel to one another, the error differential equation is as follows.

$$\frac{d}{dt} \begin{bmatrix} e_2 \\ e_3 \end{bmatrix} = \begin{bmatrix} V \sin e_3 \\ \omega - \omega_r \end{bmatrix} \quad (4)$$

We introduce a controller represented by Equation (5) with  $K_2$  and  $K_3$  as positive numbers. Here,  $\omega_r = \dot{\theta}_r + \dot{\beta}_r$  is true.

In actual control operation,  $K_2$  and  $K_3$  adopt appropriate values according to velocity and driving situation.

$$\omega_c = \omega_r - K_2 e_2 V - K_3 \sin e_3 \quad (5)$$

The target yaw rate,  $\omega_c$  cannot be directly instructed in actual control, so it is converted to the steering angle input using Equation (1) and made the control input.

$$\delta_c = \frac{MV}{2K_f} \left[ \frac{2(K_f l_f - K_r l_r)}{MV^2} \gamma + \frac{2(K_f + K_r)}{MV} \beta + \omega_r - K_2 e_2 V - K_3 \sin e_3 \right] \quad (6)$$

Various driving environments are assumed in the actual environment, and the control input represented by Equation (6) may not necessarily be appropriate in the driving situation that cannot be covered by the single track model. One of the examples is the situation in which a large steering angle is required at very low vehicle velocity such as when making a left turn at an intersection. As a countermeasure, it would be feasible to set  $K_2$  and  $K_3$  values aligned with the various driving environment. But we considered as a control it is unsuitable that controller has many  $K_2$  and  $K_3$  values aligned with various driving environments. In this development, a feed forward term of the steering angle is set predetermined value according to the travelling position, and a feedback term of the steering angle is calculated by Equation (6). The value obtained by adding both values is control input. **Figure 9** shows a block diagram for calculating the target steering motor torque.  $\theta_{TFB}$  is the value when  $\delta_c$  of Equation (6) is made the dimension of the steering wheel angle, and the feed forward term,  $\theta_{TFF}$ , is added to make the target steering angle ( $\theta_T$ ). The target steering motor torque,  $T_m$ , is calculated by the angle control to eliminate the deviation,  $\Delta\theta$ , of the target steering wheel angle,  $\theta_T$ , and the actual steering wheel angle  $\theta$ .

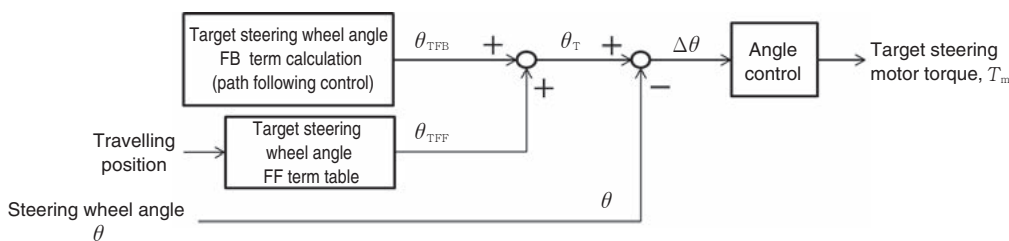


**Fig. 9** Steering control calculation

In the field operational tests, vehicle position was mainly recognized by receiving RTK-GNSS (Real Time Kinematic - Global Navigation Satellite System) signal, and steering control was implemented. The method of calculating the lateral deviation,  $e_2$ , and yaw angle deviation,  $e_3$ , used for target steering angle FB term calculation (path following control, Equation (6)) from the GNSS signal is described in the Cabinet Office 2018 Report<sup>4)</sup>, and omitted in this report.

#### 4. 1. 1 Control Considering Response Delay of Steering System

Steering system (from steering wheel angle to tire steering angle) includes elements of play (dead zone). Particularly, the amount of the play of large vehicles is considered to be larger than that of passenger cars due to the meshing of the ball screw, complexity of the linkage, etc. **Figure 10** shows the tire steering angle response to steering wheel angle in a large bus similar to **Fig. 3**<sup>3)</sup>. In order to make it easy to compare with the steering wheel angle, the tire steering angle in figure is a conversion value calculated by multiplying the steering gear ratio to the tire steering angle estimated from the tie rod displacement. The response of the tire steering angle relative to the steering wheel angle can be expressed in the backlash model, and in the vehicle in **Fig. 10** had a play equivalent to a steering wheel angle of 11 deg<sup>3)</sup>.

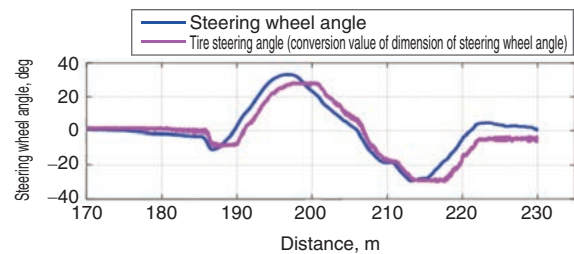


**Fig. 10** Tire angle response to steer angle

There is a concern that control may deteriorate due to the influence of play in a steering system. In particular, in a gentle turning close to travelling straight, the target steering wheel angle FB term (Equation 6) of **Fig. 9**

was relatively small, the response of the tire steering to steering was delayed, and the target vehicle behavior was not realized. In order to solve this problem, we implemented a control using the tire steering angle.

Figure 11 shows a block diagram of a control using a tire steering angle (hereinafter, tire angle control). The difference from the steering wheel angle control calculation (hereinafter, steering angle control) is expressed in blue in Fig. 9. In this control, the steering wheel angle is changed to the tire steering angle, and the motor torque is calculated by the angle control to eliminate the deviation of the target tire steering angle and the actual tire steering angle. Below is a detailed description of tire angle control compared with steering angle control.

① Target tire steering angle FB term calculation (Path Following control)

Perform the same calculation as the target steering wheel angle feedback term of steering angle control,  $\theta_{TFB}$ , and make the acquired value the target tire steering angle feedback term,  $\delta_{TFB}$ .

② Target tire steering angle FF term table

In steering angle control, the target steering wheel angle FF term table was determined based on the steering wheel angle data when traveling the route in advance. In this control, the tire steering angle conversion value is calculated using the backlash model while acquire the steering wheel angle data during traveling the route in advance, and the target tire steering angle FF term table was created based on that value. At the time of control, the output from this table is made the target tire steering angle feed forward term,  $\delta_{TFF}$ .

③ Actual tire steering angle calculation, angle deviation calculation

At the time of control, the tire steering wheel angle is estimated from the steering wheel angle using the same backlash model as used for the aforementioned tire steering angle estimation. Its value is the tire steering angle conversion value,  $\delta$ . The target steering motor torque,  $T_m$ , is calculated in accordance with the angle control to eliminate the deviation,  $\Delta\delta$ , of the target tire steering angle,  $\delta_T$ , and the actual tire steering angle,  $\delta$ . This calculation is the same that for the steering angle

control, and the control input changes from steering wheel angle deviation,  $\Delta\theta$ , to tire steering angle deviation,  $\Delta\delta$ .

Below describes the stability during straight travel as a remarkable effect of the tire angle control. Under the driving conditions shown in Table 2, steering angle control and tire angle control were compared. In this course, vehicle was driven straight to the northwest, then turned gently to the right direction and was driven straight to the north-northeast direction. Figure 12 shows one example of the results of lateral deviation and steering wheel angle during steer angle control and tire angle control. (d) shows the tire steering angle conversion value in addition to steering wheel angle. (a), (c) is the result of the same travel using steering angle control, while (b), (d) is the result of the same travel using tire angle control. As a reference, the wind direction was west and the wind speed was 3 m for (a) and (c), while for (b) and (d) the wind direction was northwest, and the wind speed was 6 m. Wind speed and direction are measured every hour at the nearest observation point (about 4 km north) from the experiment site<sup>7)</sup>. A comparison of the items in Table 3 was made in order to compare the robustness of both controls. The lateral deviation relative to the target trajectory is calculated every 0.1 m of travel distance, and the mean value, standard deviation, and  $3\sigma$  are calculated with this value. In addition, the wind speed and direction information during each trial is shown in Table 4<sup>7)</sup>.

Table 2 Experimental condition

Road shape [Direction]	Gentle right turn (R:1 500 m or above) - straight [Northwest direction - (right turn) - north-northeast direction]	
Speed, km/h	40 – 60	
Operation	Steering	Automatic control
	Accelerator	Driver
	Brake	No action

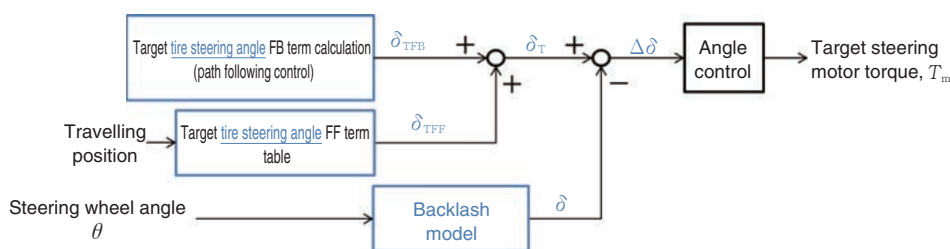


Fig. 11 Tire angle control

**Table 3** Evaluation items

Evaluation items	Mean value, standard deviation, $3\sigma$ of lateral deviation relative to the target trajectory
Number of trials	5 times each *1 500 m each time – Total 7 500 m

**Table 4** Wind information

Steering angle control			Tire angle control		
No.	Wind direction	Wind speed, m/s	No.	Wind direction	Wind speed, m/s
1	North	2	1	Southwest-south	7
2	West	3	2	Southwest-south	5
3	East	2	3	West	3
4	East	3	4	West-northwest	5
5	Northeast	2	5	Northwest	6

**Table 5** Results of lateral deviation

Item	Unit	Steering angle control	Tire angle control
Mean value	m	0.16	0.03
Standard deviation	m	0.17	0.11
$3\sigma$	m	0.51	0.33

**Figure 13** shows the distribution of the lateral deviation. **Table 5** shows the results of the lateral deviation mean value, standard deviation, and  $3\sigma$  relative to the target trajectory.

**Table 5** shows that the mean value of the lateral deviation, standard deviation, and  $3\sigma$  were improved by the tire angle control. In **Fig. 13**, it can be seen that the lateral deviation distribution of tire angle control is more distributed around zero and controlled near the target value compared to steering angle control. From the wind speed and direction information of **Table 4**, it is assumed that the wind speed is higher during tire angle control than during steering angle control. Despite the large disturbance, the tire angle control showed higher control performance than steering angle control, and robustness was improved.

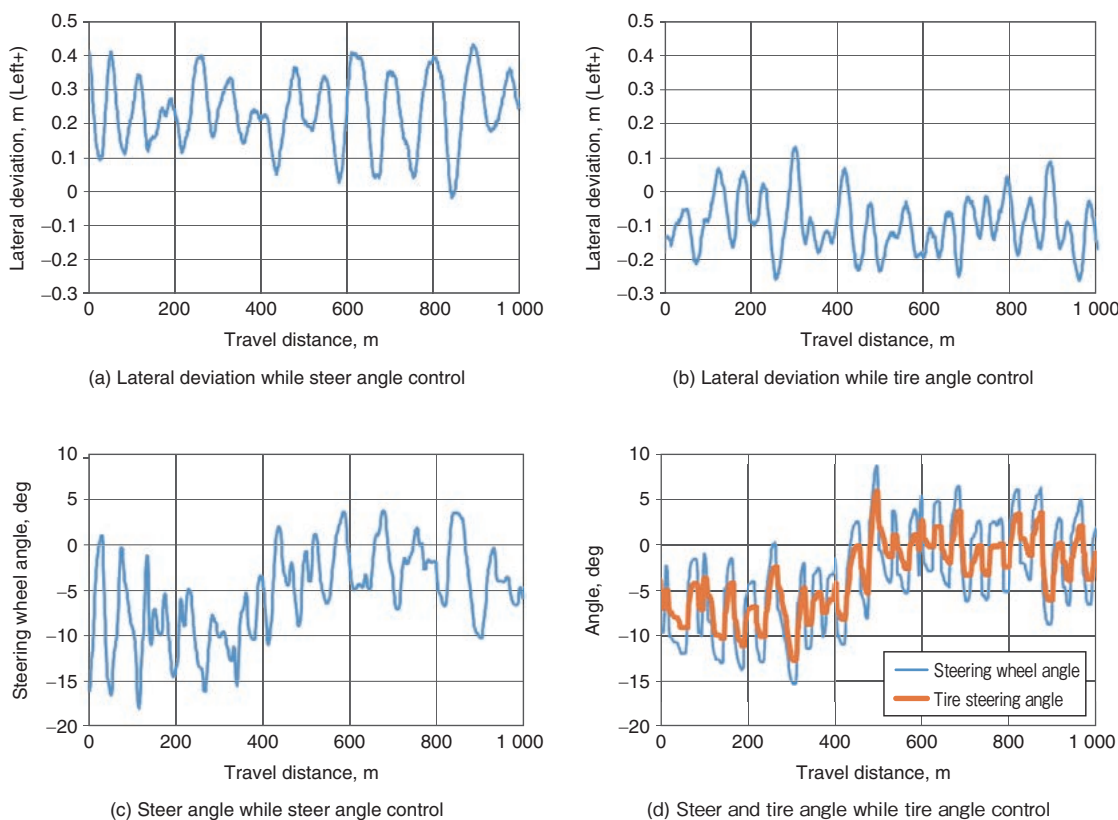


**Fig. 12** Lateral deviation and steer angle

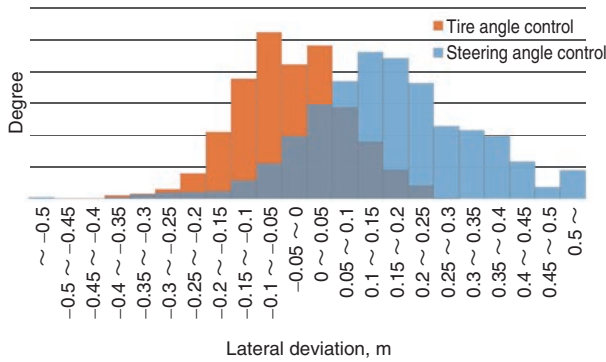


Fig. 13 Distribution of lateral deviation

The experiment vehicle (Fig. 3) has a width of 2.49 m. Assuming a normal lane width of 3.25 m, it is necessary to keep the lateral deviation within  $\pm 0.38$  m in order to travel in the lane. From the mean value and  $3\sigma$  of Table 5, there is a possibility that the steering angle control cannot keep in the lane, on the other hand, the tire angle control could keep in the lane.

4. 2 Braking Control

The braking control ECU received deceleration instruction from the integrated control system. As a characteristic of the braking system, it is necessary to deal with the variation in the actual deceleration relative to the target deceleration, and the fact that the vehicle speed at the beginning of brake application will not be constant in a real traffic environment. In order to achieve high stop position accuracy under such conditions, the target deceleration,  $a$ , is obtained from the information of the target stop position and the travelling position as per Equation (7).

$$a = \frac{v^2}{2\Delta S} \tag{7}$$

$a$ : target deceleration,  $\Delta S$ : expected stop distance, and  $v$ : vehicle speed

As shown in Fig. 14, the expected stop distance,  $\Delta S$ , is obtained by adding the distance between the two points (the target stop position and the actual position) to the distance calculated from the correction distance table. More specifically, when vehicle is far from the target stop position and it is desirable to apply weak braking, the correction distance value is large. And the value is zero near the stop position.

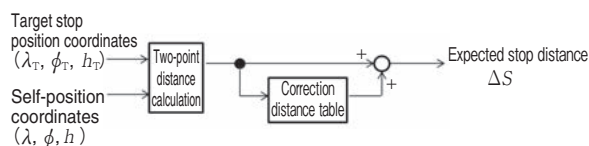


Fig. 14 Calculation of estimated stop distance

In this control, the target is not speed but deceleration calculated from the actual vehicle speed and the travelling position, so it is always suited to the driving situation. In addition, it is considered the jerk is small because the value of target deceleration is continuous.

4. 3 Precise Docking Performance during the Field Operational Tests

An example of precise docking in a large-scale field operational test carried out in the Tokyo Bay Area (Figure 1: Near Ariake Tennis-no-Mori Station) is shown. Figure 15 shows the precise docking point and the travel trajectory in the north direction near Ariake Tennis-no-Mori Station. Target trajectory is a trajectory that runs in a straight line of about 40 m after approaching width-wise about 3.8 m from the second lane in the direction of the curb.

Figure 16 shows an example of the travel trajectory in actual travel. Figure 17 shows the time series data at that time. We switched to automatic steering at the start time of Fig. 17 and performed automatic braking from around the 44 second mark. In addition, ① and ② of Fig. 16 and Fig. 17 are the same timing. The longitudinal and lateral accelerations are low until just before the stop, but the deceleration at the time of stopping is slightly large.

The target position of the lateral direction at the stop was set so that the vehicle door was a distance of 300mm from the curb. Since the aim is to keep lateral deviation (the lateral deviation of the actual position relative to the target position) within  $\pm 20$ mm during precise docking, the range of 280mm to 320mm is acceptable. Figure 18 shows the distribution of the precise docking results. The tolerance range for lateral deviation was satisfied. In terms of the longitudinal direction, the stop position also satisfied the control target (within the range of  $\pm 0.5$  m).

In the precision docking location other than the north direction of Ariake Tennis-no-Mori station, it was possible to show controllability as per the target in most cases.

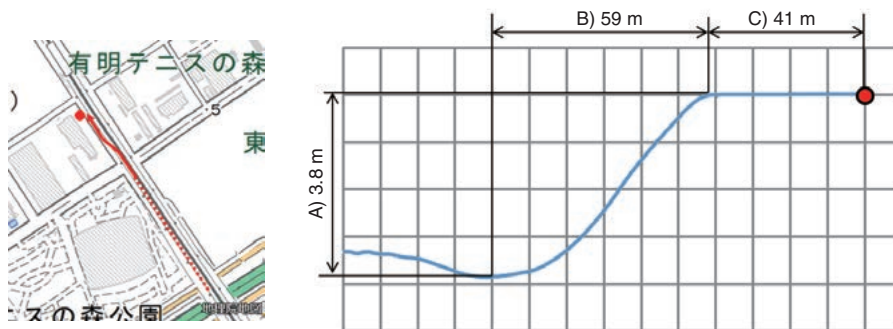


Fig. 15 Docking point near Ariake-tennis-no-mori station

\* This map is created by JTEKT Corporation based on "GSI maps" published by the Geospatial Information Authority of Japan.

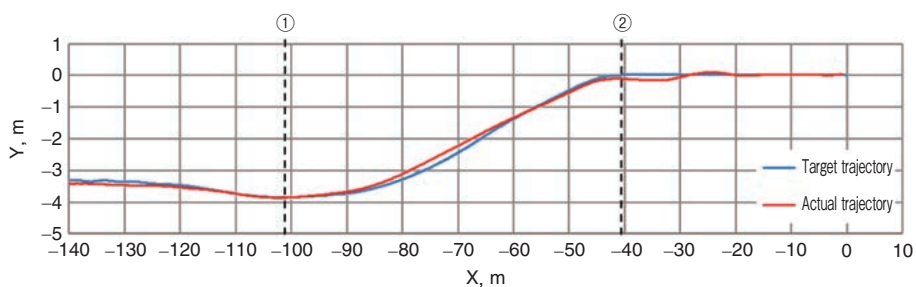


Fig. 16 Docking trajectory

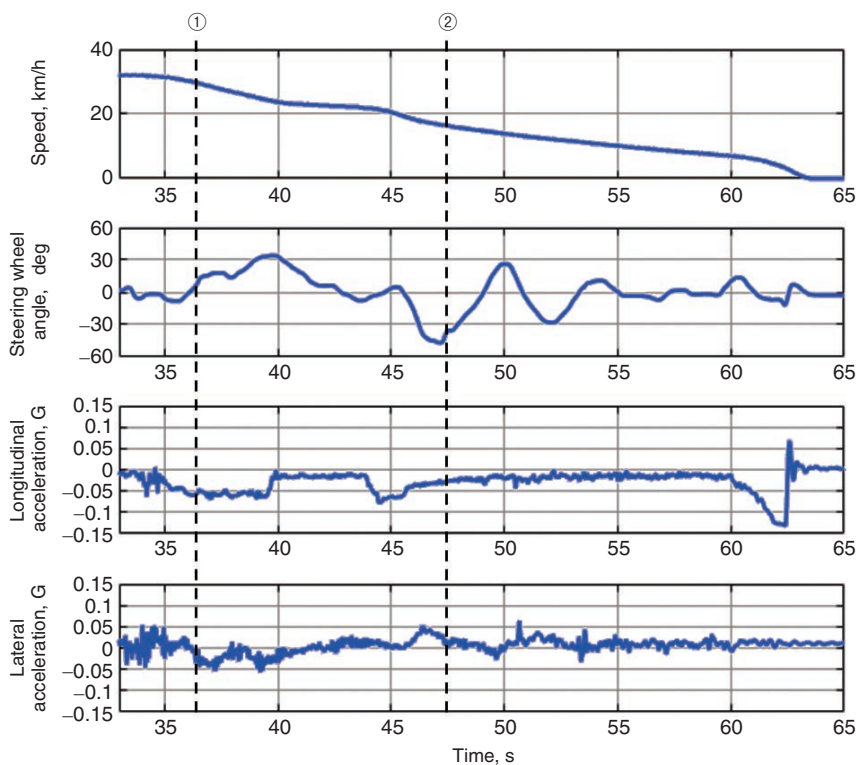
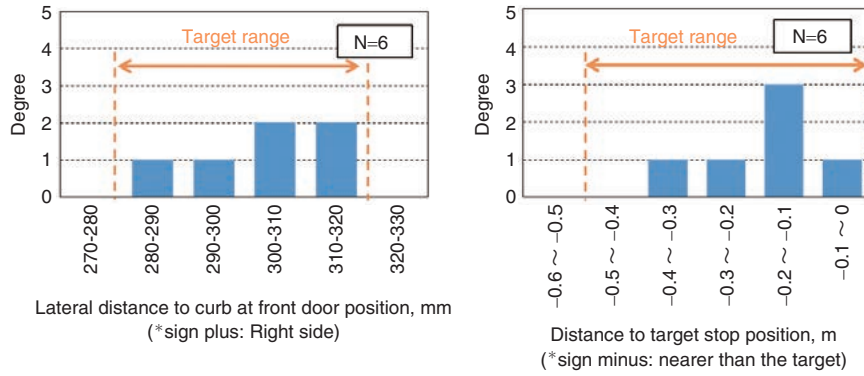


Fig. 17 Vehicle behavior while docking



**Fig. 18** Distribution of precise docking

## 5. Conclusion

In this paper, we reported the autonomous driving control technology (precise docking technology) in large buses developed as part of the Cabinet Office-led initiative, SIP “Automated Driving Systems”. We established steering and braking control, and realized precise docking with automatic steering and braking. In addition, we developed a control considering the response delay of a steering system, and realized high robustness in various environments. In the future, we will contribute to the early practical realization of these technologies by further improving the controllability and further enhancing the robustness against driving environment by utilizing sensors other than GNSS, such as cameras and LiDAR.

## References

- 1) SIP-adus’s projects (FY 2017) (ver. 31), [https://www8.cao.go.jp/cstp/gaiyo/sip/iinkai/jidousoukou\\_33/siryos33-1-1.pdf](https://www8.cao.go.jp/cstp/gaiyo/sip/iinkai/jidousoukou_33/siryos33-1-1.pdf) (in Japanese).
- 2) Cabinet Office SIP-adus’s Project (FY2016), <http://en.sip-adus.go.jp/rd/h28/project.html>  
: Next generation Transport, Investigation about actuators and control for advanced rapid transit system in investigation and consideration about issues towards autonomous driving system, [http://en.sip-adus.go.jp/wp/wp-content/uploads/project\\_2016\\_cao1-10.pdf](http://en.sip-adus.go.jp/wp/wp-content/uploads/project_2016_cao1-10.pdf)
- 3) Cabinet Office SIP-adus’s Project (FY2017), <http://en.sip-adus.go.jp/rd/>  
: Next Generation Transport, Development of Sensing and Control Technology for Docking of Advanced Rapid Transit System, [http://en.sip-adus.go.jp/file/151s\\_s.pdf](http://en.sip-adus.go.jp/file/151s_s.pdf)
- 4) Cabinet Office SIP-adus’s Project (FY2018), <http://en.sip-adus.go.jp/rd/>  
: Next-Generation Urban Transportation, Development of Sensing and Control Technology for Precise Docking of Advanced Rapid Transit system.  
\*This is a project commissioned by New Energy and Industrial Technology Development Organization (NEDO), which is the management organization of SIP-adus.
- 5) Cabinet Office SIP-adus, <http://www.sipadus.go.jp/rd/>  
: Investigation concerning automated driving bus in Okinawa (in Japanese).
- 6) T. SUGIMACHI, S. LEE, F. MOMIYAMA, Y. SUDA: Basic Study on Precision Docking based on Path Following Control, Society of Automotive Engineers of Japan, 2015 JSAE Annual Congress (Spring) proceedings, (2015) 419-424.
- 7) WEATHERNEWS INC. <http://weathernews.jp/observation/>



K. OKADA \*



M. NAKA \*



S. KAWAHARA \*\*

\* Autonomous Driving System Development Office, Steering Systems Business Unit

\*\* R&D Planning Dept., Research & Development Division